Universality of market superstatistics

Mateusz Denys, Tomasz Gubiec, Ryszard Kutner, Maciej Jagielski, and H. Eugene Stanley

Universality of market superstatistics

Mateusz Denys, Tomasz Gubiec, and Ryszard Kutner

Faculty of Physics, University of Warsaw, Pasteur Str. 5, PL-02093 Warsaw, Poland

Maciej Jagielski*

Department of Management, Technology and Economics,
ETHZ, Scheuchzerstrasse 7, CH-8092 Zürich, Switzerland
Faculty of Physics, University of Warsaw, Pasteur Str. 5, PL-02093 Warsaw, Poland and
Center for Polymer Studies and Department of Physics,
Boston University, Boston, MA 02215 USA

H. Eugene Stanley

Center for Polymer Studies and Department of Physics,
Boston University, Boston, MA 02215 USA

We use a key concept of the continuous-time random walk formalism, i.e., continuous and fluctuating interevent times in which mutual dependence is taken into account, to model market fluctuation data when traders experience excessive (or superthreshold) losses or excessive (or superthreshold) profits. We analytically derive a class of "superstatistics" that accurately model empirical market activity data supplied by Bogachev, Ludescher, Tsallis, and Bunde that exhibit transition thresholds. We measure the interevent times between excessive losses and excessive profits and use the mean interevent discrete (or step) time as a control variable to derive a universal description of empirical data collapse. Our dominant superstatistic value is a power-law corrected by the lower incomplete gamma function, which asymptotically tends toward robustness but initially gives an exponential. We find that the scaling shape exponent that drives our superstatistics subordinates itself and a "superscaling" configuration emerges. Thanks to the Weibull copula function, our approach reproduces the empirically proven dependence between successive interevent times. We also use the approach to calculate a dynamic risk function and hence the dynamic VaR, which is significant in financial risk analysis. Our results indicate that there is a functional (but not literal) balance between excessive profits and excessive losses that can be described using the same body of superstatistics, but different calibration values and driving parameters. We also extend our original approach to cover empirical seismic activity data (e.g., given by Corral) the interevent times of which range from minutes to years. Superpositioned superstatistics is another class of superstatistics that protects power-law behavior both for short- and long-time behaviors. These behaviors describe well the collapse of seismic activity data and capture so-called volatility clustering phenomena.

PACS numbers: 89.65 Gh, 05.40.-a, 89.75.Da

I. INTRODUCTION

Financial markets fluctuate, sometimes strongly, as traders estimate risk levels in order to maximize profit. The interevent interval between times when market returns produce excessive profits and when they produce excessive losses can be described using an element of the continuous-time random walk (CTRW) formalism, i.e., the waiting or pause-time distribution (see Refs. [1–4] and references therein).

Empirical market data on excessive profits and losses [5–8] define excessive profits as those greater than some positive fixed threshold Q and excessive losses as those below some negative threshold $-Q$.

The mean interevent (discrete or step) time, measured by the clock tick between profits/losses versus Q has been used as an aggregated basic variable. (The term "interevent time" appears in the literature under such names as "pausing time," "waiting time," "intertransaction time," "intertrade time," and "interoccurrence time" in different versions of the continuous-time random-walk formalism [4, 9–11, 13]).

Interevent times constitute a universal stochastic measurement of market activity on time scales that range from minutes to months [5, 6]. The mean interevent discrete time can be used as a control variable that produces a universal description of empirical data collapse [7], i.e., it produces the distribution of interevent times for a fixed mean interevent step time, which is a universal statistical quantity unaffected by time scale, type of market, asset, or index.

* zagielski@gmail.com

Interevent times in a multifractal structure of financial markets [10, 11] and in the single-step memory in order-book transaction dynamics [13] are foundational in the analysis of double auction market activity.

The distribution of interevent times can be described using (i) the canonical CTRW valley model (see Refs. [2, 4] and references therein), which treats time intervals as random variables and valley depths as single losses (or profits), and (ii) generalized extreme value statistics for stochastic dependent basic processes [14].

We use the extreme value theory to gain an approximate understanding of the phenomena. This theory uses the extreme type theorem (also called the three types theorem) and states that there are only three types of distributions needed to model the maximum or minimum of a set of random observations from the same distribution. In practice, if a statistical ensemble of M data sets (each of N elements) is generated from the same distribution and creates a new data set that contains the maximum values from these sets, the resulting data set can only be described (for large M and N) using one of three models, i.e., the Gumbel, Fréchet, and Weibull distributions. These models, along with the generalized extreme value distribution, are widely used in risk management, finance, insurance, economics, hydrology, material sciences, telecommunications, and many other fields that deal with extreme events.

The paper is organized as follows. In Sec. II we explain the principal goal of our work and indicate a possibility of extension of our approach to research areas far outside the social sciences. In Sec. III we describe how it agrees with empirical data and allows us to develop our formalism. In Sec. IV we develop our formalism and compare its predictions with a large body of empirical data from financial markets. Finally, in Sec. V we describe some useful applications of our formalism and provide concluding remarks.

II.   PRINCIPAL GOAL

Our goal is to model empirical data associated with single-variable statistics (see Sec. IV B for a detailed analysis), i.e., (i) the mean interevent discrete time period (or step) R_Q vs. $Q(> 0)$ between successive extreme losses, which are considered returns with absolute values that exceed a given threshold $Q(> 0)$ (for the sake of simplicity we treat losses as positive quantities), and (ii) the distribution $\psi_Q(\Delta_Q t)$ of the continuous interevent times between successive extreme losses, $\Delta_Q t$, previously de-

scribed using an ad hoc q-exponential [5]. Note that this type of distribution is one of the two pillars of the continuous-time random walk formalism. We thus systematically create a general formalism based on superstatistics for constructing a class of these distributions, which provides market superstatistics that have universality.

That our approach is superior to that based on q-distributions can clearly be seen by considering the dependence between subsequent interevent times. The results of our approach agree with empirical data and those based on q-distributions do not (see Sec. III C for details). Because no reliable empirical data associated with our study of excessive profits are available (the statistical errors are too large—see Sec. V B for details), we focus on excessive losses and use the empirical data provided in Refs. [5–8]. In addition to market empirical data, we can accurately describe seismic earthquake data at any scale [37] (see Sec. V C for details).

III.   BASIC ACHIEVEMENT

We find an analytical closed form of the mean interevent step time period R_Q between successive excessive losses $\varepsilon(> 0)$ that are greater than threshold $Q(> 0)$. We allow coupling between these losses and preceding interevent continuous time periods.

To more clearly explain R_Q we consider the binomial distribution as the simplest instructive reference case. An event or loss $-\varepsilon$ independent of other losses that has a probability p of occurring, appears on average Np times during a series of N observations. We thus find that the characteristic value of $N = 1/p$ and see on average a *single* loss during each series of N observations. This is not surprising because their dispersion around $Np = 1$ is $\sqrt{1 - p} < 1$. The variable N can be used as a counting process and is sometimes referred to as the operational time.

We identify probability p with the cumulative distribution $P(-\varepsilon \leq -Q)$. Hence $-\varepsilon \leq -Q$ can be considered an extreme event within $N(= 1/p)$ observations. Note that large N corresponds to a relatively small p value and hence to a relatively large Q value. This is supported by the range of the available empirical data (see Fig. 1 for details). Large losses are significant from both theoretical and practical points of view.

Using this identification we can compare R_Q with the step time variable N,

$$\left(\frac{R_Q}{\tau}\right)^{-1} = P(-\varepsilon \leq -Q) = \int_{-\infty}^{-Q} D(-\varepsilon)d\varepsilon, \quad (1)$$

where τ is an arbitrary calibration time (found from the fit to empirical data – see Formula (4) and Fig. 1), and $D(\varepsilon)$ is the distribution of returns. The challenge is to find this distribution.

Without loss of generality we can use the absolute value of the losses instead of their negative values,

$$P(-\varepsilon \le -Q) = P(\varepsilon \ge Q) = \int_Q^\infty D(\varepsilon)d\varepsilon. \quad (2)$$

The second equality allows us to quantify the density of returns $D(\varepsilon)$ as a basic local quantity, which we set using empirical data. This equation shows that there is no formal difference between losses and profits when both assume positive values.

From Eqs. (1) and (2) we find

$$D(\varepsilon) = -\frac{d\left(\frac{R_Q}{\tau}\right)^{-1}}{dQ}|_{Q=\varepsilon}. \quad (3)$$

We determine the distribution $D(\varepsilon)$ in an analytical form using the empirical dependence of R_Q^{-1} on Q (cf. Fig. 1).

This finding allows us to extend relations (1) – (3) to the case of dependent losses. Because of the coupling mentioned above we conclude that interevent continuous time periods can be dependent, and this is verified in Sec. III C.

A. $D(\varepsilon)$ vs. empirical data

Note that quantity R_Q can be directly obtained from empirical data. Figure 1 shows the quantity R_Q plotted vs. Q for four typical indices presented by different marks.

We found good agreement with empirical data (solid curves) by assuming R_Q in the form given by the formula in the upper branch of Eq. (4), which was derived from the q-Weibull distribution defined in the upper branch of Eq. (5),

$$\frac{R_Q}{\tau} = \begin{cases} \left(\exp_{q'}^{-(Q/\bar{\varepsilon}')^\eta}\right)^{-1}, \\ \exp_q^{Q/\bar{\varepsilon}}, \\ \exp\left((Q/\bar{\varepsilon})^\eta\right), \end{cases} \quad (4)$$

where τ is the irrelevant calibration time or scale factor of R_Q axis that differs in different branches (see Tables I – III). Here the values are $q' = \frac{1}{2-q}$, $q < 2$, $\bar{\varepsilon}' = \bar{\varepsilon}q'^{1/\eta}$, $\bar{\varepsilon}$, $\eta > 0$. Values of fit parameters q, $\bar{\varepsilon}$, and exponent η are shown in Table I. Here $\exp_q^{Q/\bar{\varepsilon}} = (1 + (1-q)Q/\bar{\varepsilon})^{\frac{1}{(1-q)}}$ is a q-exponential that tends to the usual exponential $\exp(Q/\bar{\varepsilon})$ when $q \to 1$. Values of fit parameters $\bar{\varepsilon}$ and q are shown
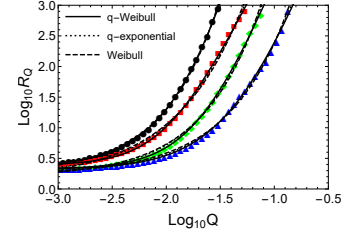

FIG. 1. Mean interevent discrete time period R_Q vs. threshold Q for four typical classes of indices. Black circles, red squares, green rhomboids, and blue triangles concern US/GBP exchange rate, S&P 500 index, IBM stock, and WTI (the crude oil) empirical data (from January 2000 to June 2010) plotted from the top down to the bottom of the figure, respectively, were taken from Fig. 2 in ref. [5]. The solid curves are the best fitted to the empirical data. These curves are predictions of the formula from the upper branch of (4) which is derived from the q-Weibull distribution. The remaining two types of curves also fit well the empirical data although slightly less accurately as previous one. Assumed resolution of the figure does not allow to distinguish (in the range of the figure) between these two types. That is, predictions of the formula from the middle branch of (4), defined by the q-exponential, are almost totally covered by predictions of the formula from the bottom branch of (4), derived from the usual Weibull distribution. Unfortunately, none of predictions are able to reproduce a weak wavy behavior of empirical data.

in Table II. This q-exponential corresponds to the distribution defined in the middle branch of Eq. (5). Table III also shows the values of $\bar{\varepsilon}$ and η driving the formula in the bottom branch, which were derived from the Weibull distribution—see the lower branch of Eq. (5).

Note that both the middle and bottom branches of Eq. (4) describe the empirical data, although slightly less accurately than the top branch. Note that middle and bottom branches are almost indistinguishable in the range of the figure. We also find an exponential distribution with predictions that differ from the empirical data.

Hence from Eqs. (3) and (4) we obtain distributions

$$D(\varepsilon) = \begin{cases} \frac{\frac{\eta}{\bar{\varepsilon}'}\left(\frac{\varepsilon}{\bar{\varepsilon}'}\right)^{\eta-1}}{1-(1-q')(\varepsilon/\bar{\varepsilon}')^\eta} \exp_{q'}^{-\left(\varepsilon/\bar{\varepsilon}'\right)^\eta}, \\ \frac{1}{\bar{\varepsilon}}\left(\exp_q^{\varepsilon/\bar{\varepsilon}}\right)^{-(2-q)}, \\ \frac{\eta}{\bar{\varepsilon}}\left(\frac{\varepsilon}{\bar{\varepsilon}}\right)^{\eta-1}\exp\left(-(\varepsilon/\bar{\varepsilon})^\eta\right). \end{cases} \quad (5)$$

These predictions are plotted in Fig. 2 for values of the corresponding parameters given in Tables I – III. Note that the q-Weibull distribution in the upper branch tends toward the usual distribution

TABLE I. Values of parameter q, exponent η, quantity $\bar{\varepsilon}$, and calibration parameter τ obtained from the fit of predictions of the top branch of Formula (4) to the empirical data (all of them plotted in Fig. 1) representing the exchange rate US Dollar against Great British Pound, the index S&P 500, the IBM stock, and crude oil (WTI).

Index/Par.	q	η	$\bar{\varepsilon}$	τ
US/GBP	1.1529±0.0085	1.267±0.0266	0.0041±0.0	2.3131±0.0333
S&P500	1.315±0.0195	1.6202±0.0869	0.0051±0.0001	2.4504±0.0689
IBM	1.2548±0.0106	1.4983±0.0398	0.0086±0.0001	2.1187±0.0267
WTI	1.2088±0.0224	1.228±0.0637	0.0131±0.0003	2.0885±0.0516

TABLE II. Values of parameters q, $\bar{\varepsilon}$, and τ obtained from the fit of predictions of the middle branch of Formula (4) to the empirical data (all of them plotted in Fig. 1) representing the exchange rate US Dollar against Great British Pound, the index S&P 500, the IBM stock, and crude oil (WTI).

Index/Par.	q	$\bar{\varepsilon}$	τ
US/GBP	0.9370±0.0051	0.0040±0.0001	1.9619±0.0302
S&P500	0.8353±0.0114	0.0048±0.0002	1.8354±0.0646
IBM	0.8969±0.0094	0.0086±0.0002	1.7404±0.0414
WTI	0.8639±0.0086	0.0146±0.0004	1.9155±0.0343

when $q' \to 1$, and the middle branch shows the usual exponential distribution when $q \to 1$.

Although q-Weibull and q-exponential distributions approximate a comprehensive analysis of the system, because multivariate q-distributions do not exist we use a two-point Weibull distribution to study the dependence of successive interevent times.

The usual Weibull distribution is used to quantify the interevent times. Reference [21] uses it to describe the statistics of interevent times between subsequent transactions for a given asset. We use it and the reinterpreted conditional exponential distribution from the CTRW valley model to derive superstatistics (or complex statistics) associated with the threshold of excessive losses or excessive profits.

Sections III B and III C describe how the usual single variable Weibull distribution is indistinguishable from the q-Weibull and q-exponential distributions.

B. An extension of the canonical EVT viewpoint

The Fisher-Tippett theorem of classical extreme value theory (the limit laws for the affine transformed maxima [17]) indicates that the cumulative distribution function (CDF) must be either Fréchet, Weibull, or Gumbel standard extreme value CDFs, but only the Weibull distribution, sometimes called a type III excessive loss [16–18], agrees with empirical data. The Fréchet and Gumbel distributions disagree with empirical data shown in Fig. 1, and thus we put them aside. Table III shows that when $\eta < 1$ the Weibull distribution for $\varepsilon/\bar{\varepsilon} \gg 1$ is a stretched
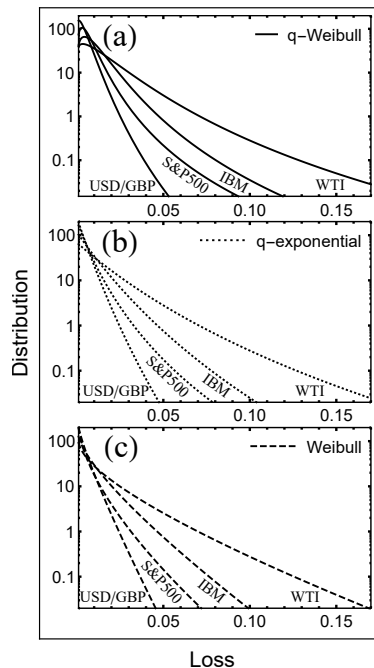

FIG. 2. Distributions, $D(\varepsilon)$ vs. ε (loss), which constituted the basis for plots in Fig. 1. The q-Weibull distribution (curves in plot (a)) only slightly differs (mainly for small losses) from the q-exponential (the corresponding curves in plot (b)) and the Weibull distributions (the corresponding curves in plot (c)). This is astonishing that q-exponential and Weibull distributions are almost indistinguishable in the interesting range of ε.

TABLE III. Values of exponent η, quantity $\bar{\varepsilon}$ and calibration parameter τ obtained from the fit of predictions of the bottom branch of Formula (4) to the empirical data (all of them plotted in Fig. 1) representing the exchange rate US Dollar against Great British Pound, the index S&P 500, the IBM stock, and crude oil (WTI).

Index/Par.	η	$\bar{\varepsilon}$	τ
US/GBP	0.8756 ± 0.0156	0.0037 ± 0.0003	1.7918 ± 0.0277
S&P500	0.6981 ± 0.0292	0.0035 ± 0.0005	1.3923 ± 0.0569
IBM	0.8246 ± 0.0236	0.0078 ± 0.0007	1.5791 ± 0.0346
WTI	0.7855 ± 0.0182	0.0131 ± 0.0008	1.7150 ± 0.0273

exponentially-truncated decreasing power-law [19].

Note that we consider random variable ε to be an increment of some underlying stochastic process. For the Weibull distribution the relative mean value $\frac{\langle\varepsilon\rangle}{\bar{\varepsilon}} = \frac{1}{\eta}\Gamma(1/\eta)$ and the relative variance $\frac{\sigma^2}{\langle\varepsilon\rangle^2} = \frac{\langle\varepsilon^2\rangle-\langle\varepsilon\rangle^2}{\langle\varepsilon\rangle^2} = \left[2\eta\frac{\Gamma(2/\eta)}{\Gamma^2(1/\eta)}-1\right]$ are η-dependent, that is, they are—for fixed exponent η—universal quantities. Bertin and Clusel [14] proved that the Fisher-Tippett theorem can be extended to strongly-dependent random variables.

C. Role of bivariate Weibull distribution

Unlike multivariate Weibull distributions, multivariate q-functions have not been found (see Eq. (5.1) in Ref. [15] for details). We thus use the bivariate Weibull distribution to construct the conditional mean interevent discrete time, $R_Q(R_{Q_0})$, i.e., we regard only the time intervals with a preceding interval length R_{Q_0}. We have

$$\frac{R_Q(R_{Q_0})}{\tau} = \left(\int_Q^\infty D(\varepsilon|Q_0)d\varepsilon\right)^{-1}, \qquad (6)$$

where the conditional distribution is defined by

$$D(\varepsilon|Q_0) \stackrel{\text{def.}}{=} \frac{\int_{Q_0}^\infty D(\varepsilon,\varepsilon_0)d\varepsilon_0}{\int_{Q_0}^\infty D(\varepsilon_0)d\varepsilon_0}$$
$$= \frac{R_{Q_0}}{\tau}\int_{Q_0}^\infty D(\varepsilon,\varepsilon_0)d\varepsilon_0, \qquad (7)$$

i.e., by the single-variate and bivariate distributions. Using Eq. (5.1) in Ref. [15] and Eqs. (6) and (7), we find the conditional mean discrete interevent time,

$$\frac{R_Q(R_{Q_0})}{\tau} = \left(\frac{R_{Q_0}}{\tau}\right)^{-1}$$
$$\times \exp\left(\left(\left(\ln\left(\frac{R_Q}{\tau}\right)\right)^{1/\gamma} + \left(\ln\left(\frac{R_{Q_0}}{\tau}\right)\right)^{1/\gamma}\right)^\gamma\right)$$
$$(8)$$

where exponent γ is a free parameter obtained from the fit of this formula to the empirical data presented

TABLE IV. Values of exponent γ and parameter τ obtained from the fit of predictions of Formula (8) to empirical data (with about 10% accuracy) for two values of R_Q and four indices (as no other data are available).

Index/Par.	$R_Q = 10$		$R_Q = 30$	
	γ	τ	γ	τ
DJIA	1.30	0.1	1.50	0.01
IBM	1.40	0.01	1.30	0.01
GBP/USD	1.37	0.001	1.27	1.0
Brent	1.25	0.0001	1.02	1.10

in Figs. 11(d) and 11(e) in Ref. [7]. The corresponding Figs. 7(d) and 7(e) – 10(d) and 10(e) concern profits. Note that based on the family of Weibull copulas the free exponent γ defines the family of bivariate Weibull distributions and not a unique distribution. In addition, when $\gamma \neq 1$ the usual multivariate Weibull distribution cannot be factored, i.e., it describes a possible dependence between interevent times. Note that only for index Brent and when $R_Q = 30$ can the subsequent interevent times be considered independent quantities (see Table IV). They otherwise are dependent, which is a result unavailable when q-functions are used.

Figure 3 compares the predictions of (8) (solid curves) with empirical data (different marks with extended error bars) from Figs. 11(d) and 11(e) in [7]. Note the extended range of R_{Q_0}/R_Q where (8) imitates a power-law dependence, and we find good agreement between our predictions and the empirical data.

IV. CLASSES OF SUPERSTATISTICS

We next construct a distribution $\psi_Q^\pm(\Delta_Q t)$ of the interevent time stochastic variable $\Delta_Q t$ in the form
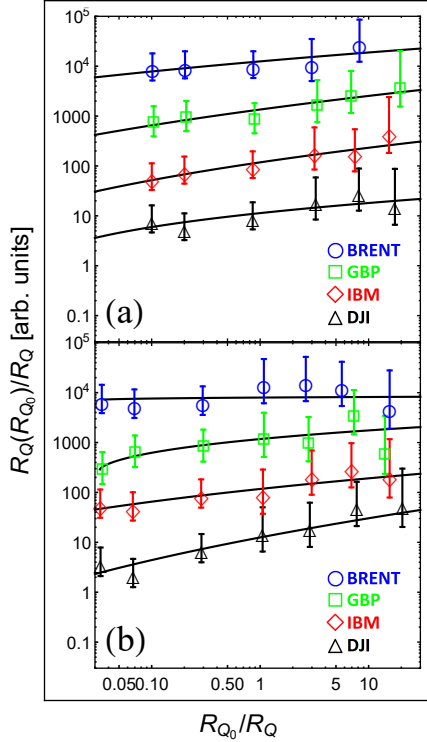
FIG. 3. Comparison of theoretical and empirical dependencies $R_Q(R_{Q_0})/R_Q$ vs R_{Q_0}/R_Q for four different indices (see legends) and two fixed values of R_Q, i.e., $R_Q = 10$ for plot (a) and $R_Q = 30$ for plot (b) (Empirical data were drawn from Fig. 7 in Ref. [7]).

of superstatistics (or complex statistics),

$$
\begin{aligned}
\psi_Q^\pm(\Delta_Q t) &= \frac{\int_Q^\infty \psi_Q^\pm(\Delta_Q t|\varepsilon) D(\varepsilon) d\varepsilon}{\int_Q^\infty D(\varepsilon) d\varepsilon} \\
&= -\frac{\int_Q^\infty \psi_Q^\pm(\Delta_Q t|\varepsilon) d\left(\int_\varepsilon^\infty D(\varepsilon') d\varepsilon'\right)}{\int_Q^\infty D(\varepsilon) d\varepsilon}.
\end{aligned}
\tag{9}
$$

We assume the conditional distribution $\psi_Q^\pm(\Delta_Q t|\varepsilon)$ in the exponential form

$$
\psi_Q^\pm(\Delta_Q t|\varepsilon) = \frac{1}{\tau_Q^\pm(\varepsilon)} \exp\left(-\frac{\Delta_Q t}{\tau_Q^\pm(\varepsilon)}\right), \tag{10}
$$

where the condition means that the next (subsequent) loss is exactly ε. The relaxation time, $\tau_Q^\pm(\varepsilon)$, is defined as a mean time-distance to this loss. If it monotonically increases with the increasing value of ε its sign is "+" and "-" if it does not. When it monotonically increases with the increasing value of ε larger losses are less frequent, and when it does

not there is volatility clustering. In general, both effects properly weighted can be present in the process. No forms of $\tau_Q^\pm(\varepsilon)$ and $D(\varepsilon)$ are used in our derivation (see Appendix A for details, where no additional constraint is assumed).

The exponential form of the conditional distribution (10) does not exclude a statistical dependence of successful interevent continuous times. In addition, because of the ε dependence of $\tau_Q^\pm(\varepsilon)$, there remains a dependence between stochastic variables ε and $\Delta_Q t$.

The subsequent step is based on a key conjecture that is valid for arbitrary $\varepsilon \geq Q$,

$$
\left(\frac{\tau_Q^\pm(0)}{\tau_Q^\pm(\varepsilon)}\right)^{\pm\alpha_Q^\pm} = \int_\varepsilon^\infty D(\varepsilon') d\varepsilon' = \left(\frac{R_{Q=\varepsilon}}{\tau}\right)^{-1},
$$
$$
\alpha_Q^\pm > 0, \tag{11}
$$

which makes an integration in the second equation in (9) feasible. We need an integration exponent $\alpha_Q^\pm$ that satisfies this equation. Its existence allows us to transform $\psi_Q^\pm(\Delta_Q t)$ into the useful form (A1). It would appear that this exponent makes the lhs of Eq. (11) Q-independent.

Equation (11) reflects the (nonlinear) general relation between the corresponding statistics of losses and the mean time distance between them. The lhs of this relation as a combined quantity is independent of the threshold variable Q, although all the individual components of this combined quantity are Q-dependent quantities. Thus we assume the existence of an integrating exponent $\alpha_Q^\pm$ that makes the lhs of Eq. (11) a Q-independent quantity and the integration in Eq. (9) feasible.

Note that Eq. (11) allows us to derive exponent $\alpha_Q^\pm$ in an explicit form when the relaxation time, $\tau_Q^\pm(\varepsilon)$, is explicitly given. Using Eq. (4) we obtain

$$
\frac{\tau_Q^\pm(\varepsilon)}{\tau_Q^\pm(0)} =
\begin{cases}
\left(\exp_{q'}^{-(\varepsilon/\bar{\varepsilon}')^\eta}\right)^{\mp 1/\alpha_Q^\pm}, & \text{for q-Weibull pdf,} \\
\left(\exp_q^{\varepsilon/\bar{\varepsilon}}\right)^{\pm 1/\alpha_Q^\pm}, & \text{for q-exp pdf,} \\
\left(\exp\left((\varepsilon/\bar{\varepsilon})^\eta\right)\right)^{\pm 1/\alpha_Q^\pm}, & \text{for Weibull pdf.}
\end{cases}
\tag{12}
$$

Assuming a stretched exponential representation typical for relaxation phenomena in disordered systems,

$$
\frac{\tau_Q^\pm(\varepsilon)}{\tau_Q^\pm(0)} = \exp\left(\pm(B_Q^\pm \varepsilon)^\eta\right), \tag{13}
$$

using Eq. (12) we obtain

$$\alpha_Q^\pm = \begin{cases} \frac{1}{(B_Q^\pm \bar{\varepsilon}')^\eta}, & \text{for q-Weibull pdf,} \\ \frac{1}{B_Q^\pm \bar{\varepsilon}}, & \text{for q-exp pdf,} \\ \frac{1}{(B_Q^\pm \bar{\varepsilon})^\eta}, & \text{for Weibull pdf,} \end{cases} \quad (14)$$

in a parametrized form for any η value, but we assume strong inequalities $|1 - q'| \ll 1$ and $|1 - q| \ll 1$ in the upper and middle branches, respectively (see Tables I and II). In Eq. (13) a more consistent approach would mean replacing the usual exp with $\exp_q$, but this would strongly complicate our approach.

The stretched exponential given by Eq. (13) is a straightforward extension of the exponential relaxation time used in the canonical CTRW valley model introduced by [1, 23–25] to describe an anomalous photocurrent relaxation in amorphous films. Quantity B_Q is a formal analog of an inverse temperature β, and is found below its scaling with the control threshold Q. Quantity $\bar{\varepsilon}$ becomes the mean valley depth.

The Weibull exponent η is present in the upper and lower branches of (12) and is the same as that used in Eqs. (4) and (5). This assumption reduces the number of free exponents (the principle of Ockham's Razor) and enables the derivation of superstatistics $\psi_Q^\pm(\Delta_Q t)$ in an exact closed analytical form.

In the canonical CTRW exponent $\eta = 1$ was set and the usual exponential distribution was assumed according to the Hopf-Arrhenius law defining the thermally activated over-barrier transitions and the Vogel-Tamm-Vulcher law used for diffusion and transport in glasses. Thus quantities $\bar{\varepsilon}$, $\bar{\varepsilon}'$, η, and $B_Q^\pm$ constitute an internal structure of combined shape exponent $\alpha_Q^\pm$ given by Eq. (14), which controls the long time-dependence of the superstatistics $\psi_Q^\pm(\Delta_Q t)$ shown below.

Note that the stochastic dependence of interevent time $\Delta_Q t$ on loss ε assumed in (10) is confirmed when smaller losses appear more frequently than larger ones. This is described by the '+' case in definition (12), where the conditional mean time at fixed ε given by $\langle \Delta_Q t \rangle_\varepsilon^+ = \tau_Q^+(\varepsilon)$ is a monotonically increasing function of ε. This creates an expanding hierarchy of interevent times where larger losses and profits appear *less* frequently than smaller ones. Unfortunately, the '-' case is examined only in Sec. V C.

Substituting (10) and the first equality in (11) into (9), we obtain superstatistics in the form (for de-

tailed derivation see Appendix A)

$$\psi_Q^\pm(\Delta_Q t) = \frac{1}{\tau_Q^\pm(Q)} \frac{\alpha_Q^\pm}{\left(\frac{\Delta_Q t}{\tau_Q^\pm(Q)}\right)^{1 \pm \alpha_Q^\pm}}$$
$$\times \Gamma^\pm\left(1 \pm \alpha_Q^\pm, \frac{\Delta_Q t}{\tau_Q^\pm(Q)}\right), \quad (15)$$

$$\Gamma^\pm\left(1 \pm \alpha_Q^\pm, \frac{\Delta_Q t}{\tau_Q^\pm(Q)}\right) = \begin{cases} \int_0^{\frac{\Delta_Q t}{\tau_Q^+(Q)}} y^{\alpha_Q^+} e^{-y} dy, \\ \int_{\frac{\Delta_Q t}{\tau_Q^-(Q)}}^\infty y^{-\alpha_Q^-} e^{-y} dy, \end{cases}$$
$$(16)$$

where $\Gamma^\pm\left(1 \pm \alpha_Q^\pm, \frac{\Delta_Q t}{\tau_Q^\pm(Q)}\right)$ are the lower ('+') and upper ('-') incomplete gamma functions, respectively. We consider the '+' and '-' cases separately because their dependence on $\frac{\Delta_Q t}{\tau_Q^\pm(Q)}$ differs.

Equation (15) asymptotically for $\frac{\Delta_Q t}{\tau_Q^+(Q)} \gg 1$ takes a power-law form

$$\psi_Q^+(\Delta_Q t) \approx \frac{1}{\tau_Q^+(Q)} \frac{\alpha_Q^+}{\left(\frac{\Delta_Q t}{\tau_Q^+(Q)}\right)^{1 + \alpha_Q^+}}$$
$$\times \Gamma^+(1 + \alpha_Q^+) \quad (17)$$

of the relative interevent time $\frac{\Delta_Q t}{\tau_Q^+(Q)}$ while initially (for $\frac{\Delta_Q t}{\tau_Q^+(Q)} \ll 1$) it takes an exponential form

$$\psi_Q^+(\Delta_Q t) \approx \frac{1}{\tau_Q^+(Q)} \frac{\alpha_Q^+}{1 + \alpha_Q^+}$$
$$\times \exp\left(-\frac{1 + \alpha_Q^+}{2 + \alpha_Q^+} \frac{\Delta_Q t}{\tau_Q^+(Q)}\right). \quad (18)$$

For exponent $\alpha_Q^+ \gg 1$, Eq. (15) reduces to the α_Q^+-independent exponential

$$\psi_Q^+(\Delta_Q t) \approx \frac{1}{\tau_Q^+(Q)} \exp\left(-\Delta_Q t / \tau_Q^+(Q)\right), \quad (19)$$

which is consistent with Eq. (18). Note that Eqs. (17) – (19) are necessary constraints that must be obeyed by any distribution claiming to describe the empirical data shown in Figs. 4 and 5.

For the opposite '-' case when $\frac{\Delta_Q t}{\tau_Q^-(Q)} \gg 1$, the corresponding relation for $\psi_Q^-(\Delta_Q t)$ in Eq. (15) becomes a power law truncated by the incomplete

upper gamma function $\Gamma^-\left(1-\alpha_Q^-, \frac{\Delta_Q t}{\tau_Q^-(Q)}\right)$. For $\frac{\Delta_Q t}{\tau_Q^-(Q)} \ll 1$ we obtain

$$\psi_Q^-(\Delta_Q t) \approx \frac{1}{\tau_Q^-(Q)} \frac{\alpha_Q^-}{\left(\frac{\Delta_Q t}{\tau_Q^-(Q)}\right)^{1-\alpha_Q^-}}$$
$$\times \Gamma^-(1-\alpha_Q^-), \quad (20)$$

which is a pure short-time power-law behavior.

A. Superscaling

We extract a scaling hypothesis for $\ln R_Q$ as the scaling variable and for Q because both are related by a one-to-one transformation (4) that allows a universal form of (15) to be solely dependent on R_Q (or Q). This variable was explored in [5] in the case of the q-exponential. Universality means that $B_Q^\pm$ present in (14) scales with Q in a power-law form or with the related scaling variable $\ln R_Q$. Thus we formulate this hypothesis as

$$B_Q^\pm = Q^\zeta \times \begin{cases} B_\pm^{1/\eta}/\bar\varepsilon'^{1+\zeta}, & \text{q-Weibull pdf,} \\ B_\pm/\bar\varepsilon^{1+\zeta}, & \text{q-exp pdf,} \\ B_\pm^{1/\eta}/\bar\varepsilon^{1+\zeta}, & \text{Weibull pdf,} \end{cases} \quad (21)$$

where prefactor $B_\pm$ and exponent ζ are Q-independent basic positive control parameters.

Thus by using (4) to replace variable Q by R_Q in (21) we can use (14) and write superscaling relations, i.e., the scaling of scaling exponent $\alpha_Q^\pm$,

$$\frac{1}{\alpha_Q^\pm} = B_\pm \times \begin{cases} \left(-\ln_{q'}\left(\frac{R_Q}{\tau}\right)^{-1}\right)^\zeta, & \text{q-Weibull pdf} \\ \ln_q^\zeta\left(\frac{R_Q}{\tau}\right), & \text{q-exp pdf} \\ \ln^\zeta\left(\frac{R_Q}{\tau}\right) & \text{Weibull pdf.} \end{cases} \quad (22)$$

The expressions in (22) are useful because they can be directly compared with empirical data, e.g., for the IBM firm, which is a typical example. From (11) we also obtain the needed relation

$$\ln\left(\frac{\tau_Q^\pm(Q)}{\tau_Q^\pm(0)}\right) = \pm\frac{1}{\alpha_Q^\pm}\ln\left(\frac{R_Q}{\tau}\right). \quad (23)$$

Note that quantities $B_Q^\pm$, $\frac{1}{\alpha_Q^\pm}$, and $\frac{\tau_Q^\pm(Q)}{\tau_Q^\pm(0)}$ all depend on the single control variable R_Q/τ. We will also consider below the R_Q-dependence of $\tau_Q^\pm(0)$ itself. Using empirical data, we examine all the above-mentioned quantities.

B. Empirical verification of our formulas

Here we empirically verify our formulas for the '+' case. We consider the '-' case in Sec. V. For the sake of simplicity we thus here omit the '$\pm$' sign.

Note that Fig. 4 and Table V show a data collapse for a given (fixed) value of a single control (aggregated) variable R_Q.

When using the Weibull distribution, the R_Q value is easier to apply than the continuous (full) mean interevent time $\langle\Delta_Q t\rangle$. Thus we use Eqs. (9) and (10), the lower branch of (5), and Eq. (13) to obtain the mth moment $\langle(\Delta_Q t)^m\rangle$, $m = 0, 1, 2, \ldots$, in an explicit closed form,

$$\langle(\Delta_Q t)^m\rangle = \int_0^\infty (\Delta_Q t)^m \, \psi_Q(\Delta_Q t) d(\Delta_Q t)$$
$$= (\tau_Q(Q))^m G_{Q,m}, \quad (24)$$

where the first equality gives the definition (here we consider only integer non-negative moments), while the key factor

$$G_{Q,m} = \frac{m!}{1 - m/\alpha_Q} \quad (25)$$

is responsible for the singular properties of $\langle(\Delta_Q t)^m\rangle$ for the '+' case, and in the '-' case no singularity appears. Here $\langle(\Delta_Q t)^m\rangle$ is finite only when $\alpha_Q > m$, and when it is not it diverges. This is in contrast to the behavior of R_Q, which, because of its quantile (not momentum) origin, is always finite. For example, for IBM $\langle\Delta_Q t\rangle$ is finite only when $R_Q \leq 10$ (see Table VI). We see an analogous situation in other, quite different indices (see Tab. V). We thus have two radically different cases, finite mean interevent continuous time, $\langle\Delta_Q t\rangle$, and infinite time—about which much appears in the literature (see, e.g., [3, 26–30] and references therein).

Figure 5 shows the somewhat more accurate fits for the IBM company, indicating an agreement between the predictions of Eq. (15) (solid curves) and the empirical data (empty circles) for $R_Q = 2, 5, 10$, 30, and 70. Table VI shows the fitted quantities α_Q and $\tau_Q(Q)$.

The detailed plots shown in Fig. 6 also concern the IBM company. Figure 6(a) shows the good fit of the Eq. (22) prediction of the q-Weibull pdf (dotted curve), the q-exponential pdf (dashed curve), and the Weibull pdf (solid curve) to the corresponding data collected from other independent fits for five values of R_Q (black circles). See also the third column of Table VI. For the sake of comparison, the corresponding values of the fitted basic quantities B and ζ are presented in Table VII for the q-Weibull, the q-exponential, and the Weibull distributions.
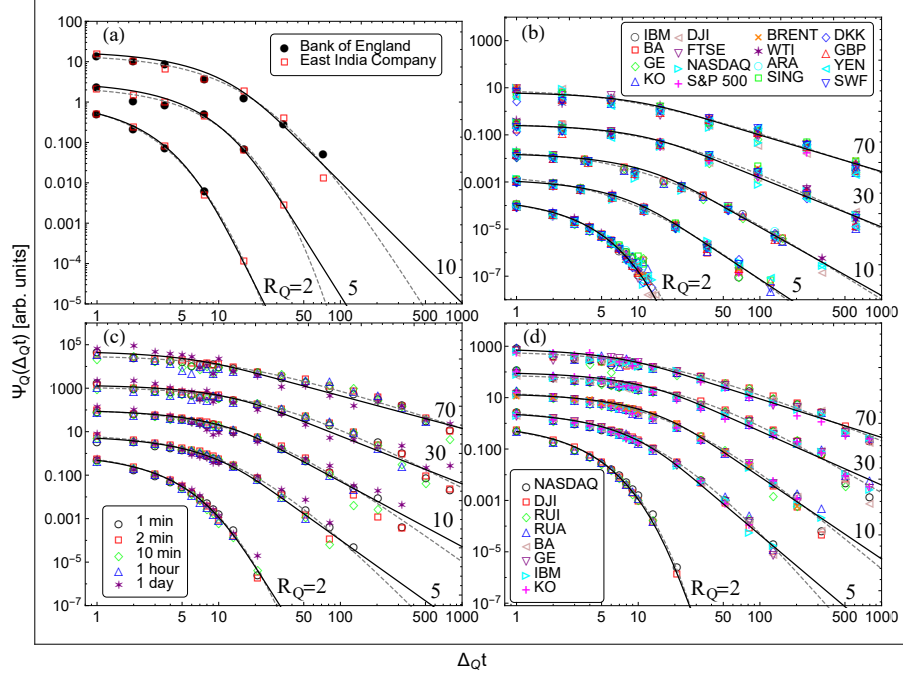
FIG. 4. Collected plots of empirical distributions (colored marks drawn from [5, 6]) and theoretical superstatistics, $\psi_Q(\Delta_Q t)$, (black solid curves), which are predictions of our Formula (15) (while the dashed curves are given by q-exponential shown by Eq. (3) in [5]) vs. interevent time, $\Delta_Q t$, for the monthly returns in the period 1709-1823 (a), for the relative daily price returns for sixteen typical examples of financial data in the period 1962-2010 (b), from minutes over the hours to daily returns for NASDAQ between March 16, 2004 and June 5, 2006 (c), and for the detrended minute-by-minute eight most typical examples of financial data (d).

TABLE V. Values of exponent α_Q and quantity $\tau_Q(Q)$ obtained from the fit of Formula (15) to the empirical data (with about 5% accuracy) representing companies shown in Fig. 4 in plots (a), (b), (c) and (d) for $R_Q =$2, 5, 10, 30, 70.

R_Q	Fig. 4(a)		Fig. 4(b)		Fig. 4(c)		Fig. 4(d)	
	α_Q	$\tau_Q(Q)$	α_Q	$\tau_Q(Q)$	α_Q	$\tau_Q(Q)$	α_Q	$\tau_Q(Q)$
2	5.0	1.15	14.0	1.27	7.8	1.256	12.2	1.34
5	3.8	3.12	2.4	2.79	3.0	2.85	3.0	2.85
10	2.0	4.58	1.9	4.6	2.0	4.39	2.20	5.09
30	-	-	1.08	5.55	1.2	5.67	1.1	5.51
70	-	-	0.55	5.39	0.5	3.5	0.5	4.08

These fits allow us to determine B and ζ and the corresponding value of the calibration parameter τ was found from an independent fit and shown in Tables II and III.

The inset plot shows the good agreement between the prediction of the lower branch of equality (21) (solid curve) and the data (black circles) obtained from the lower branch of (14). Table VI gives values of exponent α_Q for five values of Q. In like manner we compare the q-Weibull and q-exponential distri-butions.

Figure 6(b) shows a plot of $\tau_Q(Q)$ vs. Q, where $\tau_Q(Q)$ comes from the fourth column of Table VI. The plot consists of a broken straight line or two crossing straight lines. The corresponding Table VIII shows the parameters of linear regressions a_s and b_s, with $s = L, R$, that define the dependence of both straight lines on R_Q.

The inset plot uses Eq. (23) to present (i) the data points (crosses, empty squares, and black circles) of
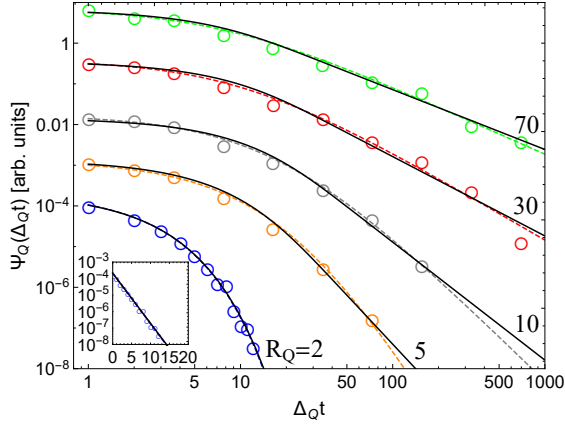
FIG. 5. The superstatistics, $\psi_Q(\Delta_Q t)$, vs. interevent time, $\Delta_Q t$, in log-log scale for the daily price returns of IBM (empty circles drawn from [5]) in the period 1962-2010 for R_Q=2, 5, 10, 30 and 70 (in units of days). Black solid curves are predictions of our Formula (15) while the dashed curves are given by q-exponential shown by Eq. (3) in [5]. For $R_Q \geq 5$ the power-law relaxation of $\psi_Q(\Delta_Q t)$ is well seen for $\Delta_Q t > 30$. The inset is the plot of $\psi_Q(\Delta_Q t)$ vs. $\Delta_Q t$ in the semi-logarithmic scale for R_Q=2 to clearly present the exponential form of the superstatistics. This exponential form was expected due to Eq. (19) as α_Q is very large in this case (see Tab. VI).

TABLE VI. Values of exponent α_Q and quantity $\tau_Q(Q)$ obtained directly from the fit of Formula (15) to the empirical data (with about 1% accuracy) representing IBM company shown in Fig. 5 for R_Q=2, 5, 10, 30, and 70.

R_Q	Q	α_Q	$\tau_Q(Q)$
2	0.0014	1000	1.4286
5	0.0093	3.0	3.33
10	0.0164	1.9	5.0
30	0.0289	0.95	4.55
70	0.0393	0.47	3.85

$\tau_Q(0)$ for five values of R_Q (as above, $\tau_Q(Q)$ is given by Table VI) and (ii) the dotted, dashed and solid curves of $\tau_Q(0)$, using the analytical form of $\tau_Q(Q)$ for arbitrary values of Q (limited by the frame of the figure).

Thus by proving the R_Q-dependence of the superstatistics $\psi_Q(\Delta_Q t)$, we explain the empirical data collapse shown in Figs. 4 and 5 and some of its consequences.

As stated in Sec. III B, the usual Weibull, the q-Weibull and q-exponential distributions provide an approximate description of single-variable empirical results and indicate that both viewpoints, i.e., extreme and non-extensive (the result of long-term
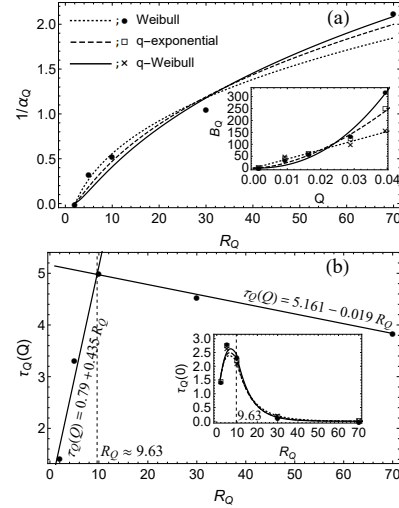

FIG. 6. Key dependence of quantities: (a) $1/\alpha_Q$ and (b) $\tau_Q(Q)$ vs. R_Q obtained, for instance, for the IBM company. Black circles in main plots represent empirical data (shown in Tab. VI), while solid curves are our theoretical predictions. The solid curve was obtained for plot (a) by the fit of Formula (22) to empirical data, where the fit parameters B and ζ were shown in Tab. VII. The indirect empirical data for the inset plot (i.e., B_Q vs. Q) were found from the lower branch of Eq. (14) by using α_Q taken from Tab. VI, while η, $\bar{\varepsilon}$ and τ from Tab. III for the IBM company. The solid curve in this inset plot is the prediction of the lower branch of Eq. (21) for mentioned above parameters B and ζ as well as η and $\bar{\varepsilon}$ taken from Tab. III. In plot (b) the broken line or both solid straight lines are linear regressions (i.e. given by $\tau_Q(Q) = a_s R_Q + b_s$, where $s = L$ for the lhs straight line and $s = R$ for the rhs straight line. In this approach we have constraint $R_Q \geq -b_R/a_R$. Herein, $\tau_{Q=0}(0) = a_L \tau + b_L$ as $R_{Q=0} = \tau$. Multiplicative and additive calibration parameters a_s and b_s defining both straight lines are shown in Tab. VIII. Thus we have an additional interpretation of $\tau_Q(Q)$ as equal R_Q up to some multiplicative and additive calibration parameters. The solid curve in the inset plot (i.e., $\tau_Q(0)$ vs. R_Q) was obtained from Formula (23), where B and ζ comes from Tab. VII, while $\tau_Q(Q)$ was defined by above given straight lines. Dotted curves (except thin vertical ones) and empty squares together with dashed curves and crosses present results obtained in the analogous way but basing on q-Weibull and q-exponential, respectively.

dependence), are closely related. We cannot exclude the possibility that they are "two sides of the same coin" and in a fluctuation-dissipation relation. There is a significant advantage to using the Weibull distribution at the level of bivariate distributions because there the q-distributions do not exist (cf. Sec.

TABLE VII. Universal parameter B and universal exponent ζ, defining dependence of B_Q vs. Q, obtained from the good fit of all formulae in (22) to the corresponding empirical data shown in Fig. 6(a), for instance, for very representative IBM company.

pdf	B	ζ
q-Weibull	0.27194±0.0685	1.0037±0.1459
q-exp	0.1572±0.0586	1.6912±0.2626
Weibull	0.1028±0.0446	2.2590±0.3393

TABLE VIII. Parameters of linear regressions a_s and b_s, $s = L, R$, defining dependence of both straight lines on R_Q (with accuracy about 1%), presented in Fig. 6(b) for the IBM company.

Parameters	L	R
a_s	0.435	-0.019
b_s	0.79	5.161

III C), i.e., q-distributions are not able to explain the dependence observed between interevent continuous times.

V. APPLICATIONS AND CONCLUDING REMARKS

We here have proposed that we can describe universality and superscaling in empirical data. Superscaling allows the possibility of classifying relaxation processes in systems, but its deeper physical meaning requires further study. We describe data collapse and daily quotations from various markets as having different time scales and use the bivariate Weibull distribution to consider the dependence of subsequent interevent times. We find that extreme events and their dependence constitute a basis sufficient for the description of threshold phenomena.

Note that using our microscopic model to simulate the behavior of agents [33, 34] we find results very close to those predicted by our central expression, Eq. (15). An approach using agent-based modeling in this context was also recently explored by other researchers [35, 36].

Our model is analogous to the one-dimensional CTRW valley model in that valley depth signifies loss or profit. Here $\psi_Q(\Delta_Q t)$ in the analytical closed form is the distribution of times between events and the probability density of finding a tagged particle in the adjacent valley with an depth greater than Q at time lag $\Delta_Q t$. This analogy with the valley model also indicates the form of exponent $\alpha_Q^\pm$ given by multibranch Eq. (14), where $B_Q^\pm$ is an analog of an

inverse temperature that also scales with Q and creates superscaling. This allows the universal control and direction of losses and profits, although exponent ζ in Eq. (21) remains an enigmatic value. Our extension of the formalism shows that both the exponential distribution and also the Weibull one model reveal the landscape of a substrate leading to a decreasing power-law of $\psi_Q(\Delta_Q t)$ for long time lags $\Delta_Q t$. The construction of $\psi_Q(\Delta_Q t)$ separately for losses and profits is the initial step in a preparation of the full CTRW formalism for financial markets. The full formalism requires a simultaneous consideration both losses and profits, and this remains a challenge.

Our research opens the possibility of applying the formalism in research fields other than finance. One example is in geophysics to describe seismic empirical data (see Sec. V C). The formalism can be applied to a broad spectrum of threshold phenomena, and we describe below two applications of our approach that are both practically and theoretically significant—see Secs. V(A) and V(B).

A. Application to risk estimation

The distribution of interevent times $\psi_Q^\pm(\Delta_Q t)$ is an essential value in financial engineering because it enables us to calculate risk.

The risk function $W_Q^\pm(t; \Delta t)$ is defined as the conditional probability that a current single loss ε greater than the threshold Q will occur within the next time interval Δt under the condition that the previous such loss occurred t days in the past. Reference [12] shows that $W_Q^\pm(t; \Delta t)$ is related to $\psi_Q^\pm(\Delta_Q t)$ by the generic formula

$$W_Q^\pm(t; \Delta t) = \frac{\int_t^{t+\Delta t} \psi_Q^\pm(\Delta_Q t) d\Delta_Q t}{\int_t^\infty \psi_Q^\pm(\Delta_Q t) d\Delta_Q t}. \quad (26)$$

Because $\psi_Q^\pm(\Delta_Q t)$ is given by (15) and both cumulative distributions by (26), the risk function can be obtained in a closed analytical form. The simple integration required by (26) yields

$$W_Q^\pm(t; \Delta t) = 1$$
$$- \frac{\frac{\Gamma^\pm(1\pm\alpha_Q^\pm,(t+\Delta t)/\tau_Q^\pm(Q))}{((t+\Delta t)/\tau_Q^\pm(Q))^{\pm\alpha_Q^\pm}} \pm \exp\left(-\frac{t+\Delta t}{\tau_Q^\pm(Q)}\right)}{\frac{\Gamma^\pm(1\pm\alpha_Q^\pm,t/\tau_Q^\pm(Q))}{(t/\tau_Q^\pm(Q))^{\pm\alpha_Q^\pm}} \pm \exp\left(-\frac{t}{\tau_Q^\pm(Q)}\right)}. \quad (27)$$

Although in principle both the '+' and '-' cases should be considered, we limit our work to the '+'
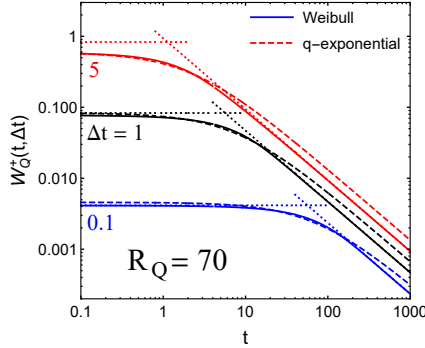
FIG. 7. Comparison of two risk functions. The solid curves are predictions of our Formula (27) based on the Weibull distribution, while the dashed curves the corresponding ones given by Formula (6a) from Ref. [5] based on q-exponential. Apparently, both formula give the same universal Zipf law behavior for the asymptotic long time t (cf. also Eq. (28)). The short-time behavior is driven by Formula (29). Predictions of both formulae are shown by dotted straight lines (oblique and horizontal asymptotes, respectively).
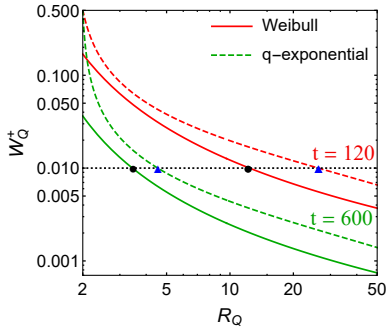
FIG. 8. Comparison of two risk functions, for two sample selected moments of time (well separated for better visualization, i.e., $t = 120$ and $t = 600$). The solid curves are predictions of our Formula (27) based on the Weibull distribution, while the dashed curves the corresponding ones given by Formula (6a) in Ref. [5] based on q-exponential, both for $\Delta t = 1.0$. The dotted horizontal line is plotted, e.g., for probability $p = 0.01$ (the confidence probability $1 - p = 0.99$). Apparently, if W_Q^+ is fixed at a given p value then, the longer time t forces a shorter value of R_Q (or Q; see the location of small circles and triangles).

case because it is able to accurately describe all the empirical data. From Eq. (27) we obtain

$$W_Q^+(t; \Delta t) \approx \alpha_Q^+ \frac{\Delta t}{t}, \ \min\left(\frac{t}{\tau_Q^+(Q)}, \frac{\Delta t}{t}\right) \gg 1. \tag{28}$$

It appears that only in an asymptotic long time does the risk function tend to a universal Zipf law irrespective of the type of market and the time horizon. On the other hand

$$W_Q^+(t; \Delta t) \approx \frac{\alpha_Q^+}{1 + \alpha_Q^+} \frac{\Delta t}{\tau_Q^+(Q)}, \ \frac{t + \Delta t}{\tau_Q^+(Q)} \ll 1, \tag{29}$$

is the time-independent quantity.

Figure 7 shows the predictions of (27) for the Weibull distribution with parameters from the IBM company for $R_Q = 70$ (solid curves) plotted versus t for three different values of Δt, which is considered a driving parameter. Note the expected asymptotic coincidence with the corresponding risk function based on the q-exponential given by Eq. (6a) in Ref. [5].

In addition, Fig. 7 shows the monotonic decreasing of the risk function versus time t at fixed Δt and R_Q, and 8 shows it versus R_Q at fixed Δt and t. These are utilized below in a numerical sampling that reveals such useful quantities for financial analysis as $|VaR|$.

The algorithm of the numerical sampling is given in Ref. [5, 7, 8]. We adapt it to our approach. To push the algorithm, the initial zero-order value of the threshold Q is required, and we obtain it by using (1), (2), and (4). Setting $P(\varepsilon \geq Q)$ equal to probability p, we have

$$Q = \begin{cases} \bar{\varepsilon}'\left(-\ln_{q'} p\right)^{1/\eta}, \\ \bar{\varepsilon}\ln_q\left(\frac{1}{p}\right), \\ \bar{\varepsilon}\left(-\ln p\right)^{1/\eta}, \end{cases} \tag{30}$$

where $\ln_q(\ldots)$ is a q-logarithm, i.e., the inverse of a q-exponential. We now can set $|VaR| = Q$ and finish this initial step.

With the zero-order threshold Q time t can be drawn as a stochastic variable from the distribution $\psi_Q^+(t = \Delta_Q t)$ given by Eq. (15). Subsequently, Q and t enable us to calculate the concrete value of risk function $W_Q^+(t; \Delta t)$ from Eq. (27) and decide whether its value falls into the band $p \pm \Delta p$ where $\Delta p \ll p$. If that is the case we can set $|VaR| = Q$ and draw the next time interval t from $\psi_Q^+(t = \Delta_Q t)$ for this value of Q. Substituting these t and Q values into Eq. (27), we obtain a new value of $W_Q^+(t; \Delta t)$.
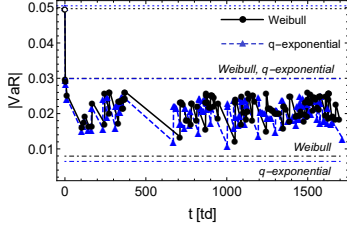
FIG. 9. Comparison of two simulated absolute Value-at-Risk time series: (i) based on the Weibull distribution (small black circles connected by segments of solid straight line) and (ii) based on q-exponential (triangles connected by segments of dashed straight line) both using our Formula (27) for $\Delta t = 0.1$. The time range of both series is as those in Fig. 6 in Ref. [5] that is, for the IBM stock between 2002 and 2008 for the confidence probability $1 - p = 0.99$. Two horizontal dotted lines (situated at an altitude of about 0.05) show the zero-order $|VaR|$ where no dependence between interevent times is present for the Weibull and q-exponential distributions, respectively. Two pairs of dashed-dotted horizontal lines show the most probable spreads of simulated $|VaR|$-s for the Weibull and q-exponential distributions, respectively. Apparently, our approach drastically reduces $|VaR|$, i.e., the level of losses, in comparison with the zero-order $|VaR|$ (the single empty circle and triangle).

When this value is outside the band $p \pm \Delta p$ we multiply Q by factor $1 \pm \gamma$ where $\gamma \ll 1$ depending on whether it is greater than $p + \Delta p$ (we then choose '+') or lower than $p - \Delta p$ (we then choose '-'), respectively. We repeat this step as many times as necessary, e.g., $n_+ + n_-$ times, to find the corresponding $Q' = Q(1 + \gamma)^{n_+}(1 - \gamma)^{n_-}$ and the value of t (analogously as given above). Both Q' and t are then substituting into Eq. (27), which gives the value of $W_{Q'}^+(t; \Delta t)$ contained in the band. We now can see that the new $|VaR|$ is equal to Q'. In this way we obtain the series of $|VaR|$-s at the proper points in time, i.e., at $(t + \Delta t)$-s. Figure 9 shows that this series consists of fluctuating values that are below the initial $|VaR|$. The most probable spread of this series, which is denoted by pairs of dashed-dotted horizontal lines in Fig. 9, occurs only over extremely long time periods.

B. Application to profit analysis

We model the empirical data collapse (cf. Fig. 4) using superstatistics $\psi_Q^+(\Delta_Q t)$ given by (15) parametrized by a single aggregated variable R_Q and obtain, for example, the scaling shape exponent

$1/\alpha_Q^+$ as a power-law function of $\ln R_Q$ and the superscaling form of (22) that is dependent upon universal exponent ζ and prefactor $B_\pm$.

Note that $\psi_Q^+(\Delta_Q t)$ also accurately describes the rescaled empirical statistics of excessive profits. Here Q defines the threshold for excessive profits instead of excessive losses (see the plots in Fig. 10). We thus can use the same superstatistics to demonstrate the functional but not literal symmetry between excessive losses and profits. The symmetry is not literal because different control parameters, i.e., exponent α_Q and relaxation time $\tau_Q(Q)$, are used. Because of large statistical errors in the empirical data, we cannot empirically verify the universality of excessive profit behavior. For example, for $R_Q = 10$ exponent $1.70 \leq \alpha_Q \leq 3.10$ and $0.10 \leq \tau_Q(Q) \leq 0.25$, for $R_Q = 30$ we have $0.90 \leq \alpha_Q \leq 1.50$ and $0.12 \leq \tau_Q(Q) \leq 0.35$, and finally for $R_Q = 70$ we have $0.60 \leq \alpha_Q \leq 1.10$ and $0.08 \leq \tau_Q(Q) \leq 0.36$, which exhibit ranges that are too extended.

C. Application to sesismic data

Another significant application of our approach is the superposition

$$\psi_Q^{tot}(\Delta_Q t) = w_Q^- \psi_Q^-(\Delta_Q t) + w_Q^+ \psi_Q^+(\Delta_Q t),$$
$$w_Q^- + w_Q^+ = 1, \quad (31)$$

based on the Weibull distribution. When $\eta = 1$ (an exponential distribution) it accurate describes the rescaled seismic empirical data [37] throughout the range of the variable 2 min. $\leq \Delta_Q t \stackrel{<}{\sim} 1.5$ year for values of Q in the range from $Q = 1.5$ to $Q = 7.5$. The notation M_c instead of Q was used in Ref. [37]. This exponential distribution leads to the widely applicable Gutenberg-Richter law that describes the frequency of earthquakes in a region with a magnitude larger than given threshold value Q. Here this law can be achieved directly as the reverse of the lower branch of Eq. (4).

Both the seismic single regions of L degrees in longitude and L degrees in latitude were taken into account as well as several other regions (see Fig. 11). Using Eq. (31) we take into account two effects, (i) the large volatility clustering described by $\psi_Q^-(\Delta_Q t)$ that causes avalanches of earthquakes or aftershock sequences, and (ii) the small volatility clustering described by $\psi_Q^+(\Delta_Q t)$ that causes weak aftershock sequences. Taking into account both effects is important although a sufficiently precise determination of w_Q^- and α_Q^- is impossible because exponent α_Q^-, although still positive, is too small. In addition, we
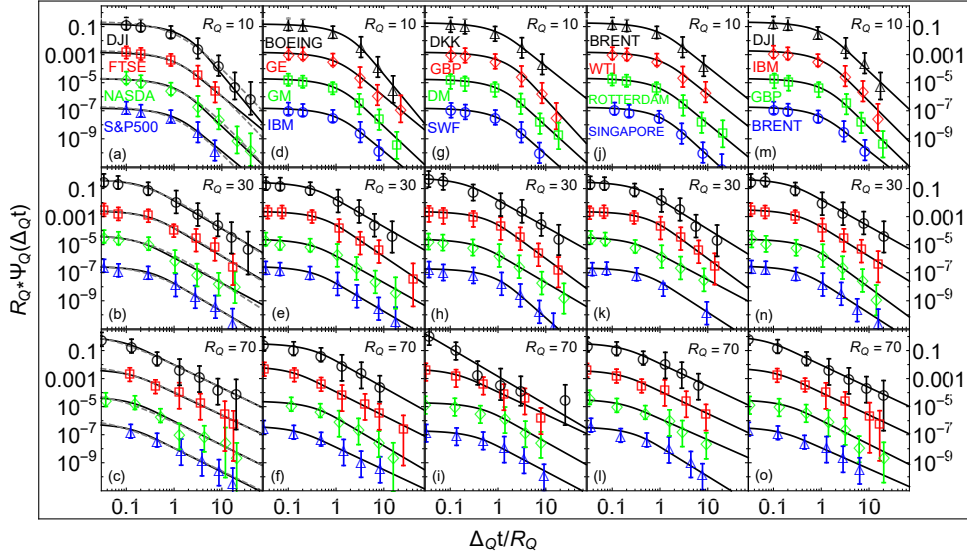
FIG. 10. Statistics of interevent times between profit returns of daily closing prices for various markets (from stock exchange and forex to resource market) and time periods. All empirical data (discrete marks with bars) were taken from ref. [7]. Solid curves are predictions of our Formula (15) as it can be applied both for losses and profits. Dashed curves shown, for instance, in plots (a), (b), and (c) are fitted by q-exponential (remaining twelve plots are very similarly fitted therefore, the fits are not visualized herein). However, the possible empirical data collapse would be incredible in this case because errors of empirical data points are too large.

see no Q-dependence of exponent $\alpha_Q^\pm$ and relaxation time $\tau_Q^\pm(Q)$. Thus it is sufficient to characterize each region, (a) – (f), using single values of exponents α_Q^-, α_Q^+ and relaxation times $\tau_Q^-(Q)$, $\tau_Q^+(Q)$ (see Table IX). Thus using Eqs. (13) and the lower branches of (14) and (21) for the decreasing value of scaling exponent ζ we write

$$\alpha_Q^\pm = (B_\pm)^{-1},$$
$$\frac{\tau_Q^\pm(Q)}{\tau_Q^\pm(0)} = \exp\left(\pm B_\pm \frac{Q}{\bar{\varepsilon}}\right), \qquad (32)$$

where constraint

$$\tau_Q^\pm(0) \propto \exp\left(\mp B_\pm \frac{Q}{\bar{\varepsilon}}\right) \qquad (33)$$

must be obeyed.

Seismic empirical data prove that scalings are a prominent feature of the earthquake mechanism, which we still do not understand. Our formula is well-suited to the empirical data because it is driven by two power laws. For short interevent times it is dominated by the Omori law [31, 32] in which ψ_Q^+ is self-damped by the upper incomplete gamma function. For long interevent times the power-law driven by Pareto-Lévy exponents greater than 2 plays the

TABLE IX. Values of ratio w_Q^-/w_Q^+, exponents $\alpha_Q^\pm$ and relaxation times $\tau_Q^\pm(Q)$ obtained directly from the fit of Formula (31) to the seismic empirical data (with accuracy about 5%) shown in Fig. 11.

Region	w_Q^-/w_Q^+	$\alpha_Q^-; \alpha_Q^+$	$\tau_Q^-(Q); \tau_Q^+(Q)$
a	90/9	0.001; 7.0	1.0; 1.0
b	1000/1	0.00001; 7.0	1.0; 1.0
c	11000/9	0.00001; 7.0	1.0; 1.0
d	1400/1	0.00001; 7.0	1.0; 1.0
e	20/12	0.005; 6.0	1.0; 0.8
f	80/11	0.001; 4.0	1.0; 0.7

most significant role in which ψ_Q^- is self-truncated by the lower incomplete gamma function—see Eqs. (15) and (16), and Fig. 11 for details.

It is our hope that this work will be a valuable contribution to the research effort searching for universal properties not confined to market behavior. The formalism we propose accurately describes the universalities in empirical data and allows us to classify quotes using a single scaling variable that points out their similarities. These similarities suggest that there is a root cause underlying the identical shape of various distributions of interevent times in different time scales. This should allow us to finally derive,
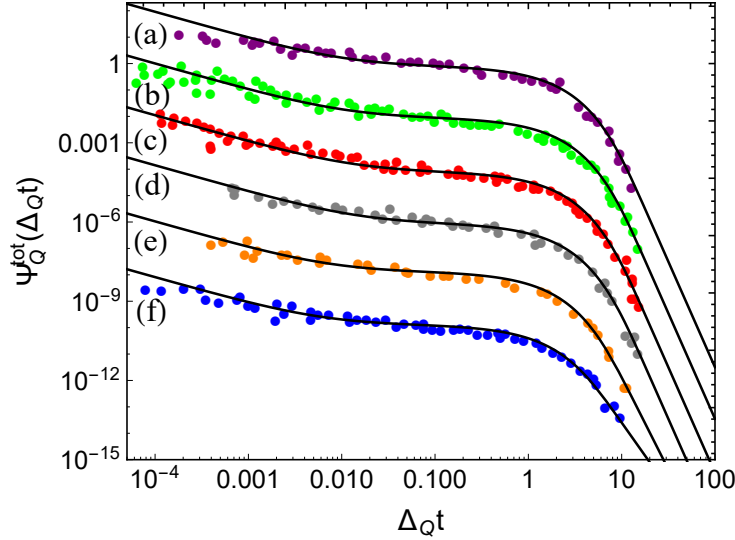
FIG. 11. Six rescaled statistics (representing Bak et al.'s unified scaling law for earthquakes), for the single-region seismic empirical data (small circles), of interevent times between successive earthquakes of magnitude stronger than the corresponding well defined thresholds (from 1.5 to 7.5 in the Richter scale). The seismic single regions are as follows: (a) the NEIC worldwide catalog for regions with $L \geq 180°$ for years 1973-2002, (b) NEIC with $L \leq 90°$ (the same years), (c) Southern California years 1984-2001, 1988-1991, and 1995-1998, (d) Northern California years 1998-2002, (e) Japan 1995-1998 and New Zealand 1996-2001, (f) Spain years 1993-1997, New Madrid 1975-2002, and Great Britain years 1991-2001. The interevent times go from 2 min. to about 1.5 years. Empirical curves (small circles) were drawn from [37] – they are spreaded vertically for better visibility. Solid curves are predictions of Formula (31) describing well these rescaled empirical statistics, which collapse well for different regions and values of threshold Q.

for example, *ab initio* equations describing financial market behavior.

Appendix A: Derivation of $\psi_Q^{\pm}(\Delta_Q t)$

To derive the distribution $\psi_Q^{\pm}(\Delta_Q t)$ we use the second equality in Eq. (9),

$$\psi_Q^{\pm}(\Delta_Q t) = -\frac{\int_Q^\infty \psi_Q^{\pm}(\Delta_Q t|\varepsilon) d\left(\int_\varepsilon^\infty D(\varepsilon')d\varepsilon'\right)}{\int_Q^\infty D(\varepsilon)d\varepsilon},$$

which we will then use in further transformations.

We base our next step on Eq. (11), which enables us to rewrite above equality in the form

$$\psi_Q^{\pm}(\Delta_Q t) = \frac{1}{z(Q)}\frac{1}{\tau_Q(0)}I_Q^{\pm}, \qquad (A1)$$

where auxiliary variable

$$z = z(\varepsilon) \stackrel{\text{def.}}{=} \int_\varepsilon^\infty D(\varepsilon')d\varepsilon' \qquad (A2)$$

and integral

$$I_Q^{\pm} \stackrel{\text{def.}}{=} \int_0^{\tau R_Q^{-1}} z^{\pm 1/\alpha_Q^{\pm}} \exp\left(-z^{\pm 1/\alpha_Q^{\pm}}\frac{\Delta_Q t}{\tau_Q^{\pm}(0)}\right) dz$$

$$= A_Q^{\pm} \int_0^{\tau R_Q^{-1}} exp\left(-z^{\pm 1/\alpha_Q^{\pm}}\frac{\Delta_Q t}{\tau_Q^{\pm}(0)}\right) d\left(z^{1\pm 1/\alpha_Q^{\pm}}\right)$$

where $A_Q^\pm = \frac{1}{1 \pm 1/\alpha_Q^\pm}$. By using the identity

$$d\left(z^{1 \pm 1/\alpha_Q^\pm}\right) = d\left(z^{\pm 1/\alpha_Q^\pm} \frac{\Delta_Q t}{\tau_Q^\pm(0)}\right)^{\alpha_Q^\pm(1/\alpha_Q^\pm \pm 1)}$$
$$\times \left(\frac{\tau_Q^\pm(0)}{\Delta_Q t}\right)^{1 \pm 1/\alpha_Q^\pm} \tag{A3}$$

we finally obtain from Eq. (A1) with help of Eqs. (A2) and (A3),

$$\psi_Q^\pm(\Delta_Q t) = \frac{1}{\tau_Q^\pm(Q)} \frac{\alpha_Q^\pm}{\left(\Delta_Q t/\tau_Q^\pm(Q)\right)^{1 \pm \alpha_Q^\pm}}$$
$$\times \Gamma^\pm\left(1 \pm \alpha_Q^\pm, \frac{\Delta_Q t}{\tau_Q^\pm(Q)}\right), \tag{A4}$$

where

$$\Gamma^+\left(1 + \alpha_Q^+, \frac{\Delta_Q t}{\tau_Q^+(Q)}\right) = \int_0^{\frac{\Delta_Q t}{\tau_Q^+(Q)}} u^{\alpha_Q^+} \exp(-u) du$$

is the lower incomplete gamma (Euler) function, where we change the variables

$$u \stackrel{\text{def.}}{=} z^{1/\alpha_Q^+} \frac{\Delta_Q t}{\tau_Q^+(0)} \tag{A5}$$

and

$$\Gamma^-\left(1 - \alpha_Q^-, \frac{\Delta_Q t}{\tau_Q^-(Q)}\right) = \int_{\frac{\Delta_Q t}{\tau_Q^-(Q)}}^\infty u^{-\alpha_Q^-} \exp(-u) du,$$

is the upper incomplete gamma (Euler) function. We change the variables such that they are complementary to (A5),

$$u \stackrel{\text{def.}}{=} z^{-1/\alpha_Q^-} \frac{\Delta_Q t}{\tau_Q^-(0)}. \tag{A6}$$

Hence

$$d\left(u^{1 \pm \alpha_Q^\pm}\right) = (1 \pm \alpha_Q^\pm) u^{\pm \alpha_Q^\pm} du \tag{A7}$$

is used in both '+' and '−' cases.

---

[1] G. Pfister and H. Scher, *Adv. Phys.* **27**, 747 (1978).
[2] J. W. Haus and K. W. Kehr, *Phys. Rep.* **150**, 263 (1987).
[3] R. Kutner and F. Świtała, *Quant. Finance* **3**, 201 (2003).
[4] T. Sandev, A. Chechkin, H. Kantz, R. Mentzler, *An Int. J. Theory and Applications* **18**, 1006 v(2015).
[5] J. Ludescher, C. Tsallis, A. Bunde, *Eur. Phys. Let.* **95**, 68002 (2011).
[6] J. Ludescher and A. Bunde, *Phys. Rev. E* **90**, 062809 (2014).
[7] M. I. Bogachev and A. Bunde, *Phys. Rev. E* **78**, 036114 (2008).
[8] M. I. Bogachev and A. Bunde, *Phys. Rev. E* **80**, 026131 (2009).
[9] K. W. Kehr, R. Kutner, K. Binder, *Phys. Rev. B* **23**, 4931 (1981).
[10] J. Perelló, J. Masoliver, A. Kasprzak, and R. Kutner, *Phys. Rev. E* **78**, 036108 (2008).
[11] A. Kasprzak, R. Kutner, J. Perelló, J. Masoliver, *Eur. Phys. J. B* **76**, 513 (2010).
[12] M.I. Bogachev, J.F. Eichner, A. Bunde, *Phys. Rev. Lett.* **99**, 240601 (2007).
[13] T. Gubiec and R. Kutner, *Phys. Rev. E* **82**, 046119 (2010).
[14] E. Bertin and M. Clusel, *J. Phys. A: Math. Gen.* **39**, 7607 (2006).
[15] L. Lee, J. Multivariate Anal. 9(2), 267 (1979).
[16] Y. Malevergne and D. Sornette, *Extreme Financial Risks. From Dependence to Risk Management* (Springer-Verlag, Berlin, 2006).
[17] P. Embrechts, C. Klüppelberg C., Th, Mikosch, *Modelling Extremal Events for Insurance and Finance* (Springer-Verlag, Berlin, 1997).
[18] J. Franke, W. Härdle, Ch. Hafner, *Statistics of Financial Markets*, (Springer-Verlag, Berlin, 2004).
[19] B. B. Mandelbrot, *Fractals and Scaling in Finance* (Springer-Verlag, New York, 1997).
[20] C. Tsallis, *J. Stat. Phys.* **52**, 479 (1988).
[21] P. Ch. Ivanov, A. Yuen, B. Podobnik, Y. Lee, *Phys. Rev. E* **69**, 056107 (2004).
[22] C. Tsallis, arXiv:1601.03688v1 [cond-mat.stat-mech] 14 Jan 2016.
[23] E. W. Montroll and G. H. Weiss, *J. Math. Phys.* **6**, 167 (1965).
[24] G. H. Weiss, *Aspects and Applications of the Random Walk* (North-Holland, Amsterdam, 1994).
[25] H. Scher and E. W. Montroll, *Phys. Rev. B* **12**, 2455 (1975).
[26] J. H. P. Schulz and E. Barkai, *Phys. Rev. E* **91**, 062129 (2015).
[27] R. Kutner and M. Regulski, *Physica A* **264**, 84 (1999).
[28] R. Kutner and M. Regulski, *Physica A* **264**, 107 (1999).
[29] G. Bel and E. Barkai, *Phys. Rev. Lett.* **94**, 240602 (2005).
[30] G. Bel and E. Barkai, *Phys. Rev. E* **73**, 016125 (2006).
[31] Y. Fujiwara, *Omori Law After Exogenous Shocks on Supplier-Customer Network* in *Econophysics of Systemic Risk and Network Dynamics* by F. Abergel, B.

K. Chakrabarti, A. Chakraborti, A. Ghosh (Eds.) (Springer-Verlag, Milan 2013), p. 39.

[32] F. Baldovin, F. Camana, M. Caraglio, A.L. Stella, and M. Zamparo, *Aftershock Prediction for High-Frequency Financial Markets* in *Econophysics of Systemic Risk and Network Dynamics* by F. Abergel, B. K. Chakrabarti, A. Chakraborti, A. Ghosh (Eds.) (Springer-Verlag, Milan 2013), p. 49.

[33] M. Denys, T. Gubiec, R. Kutner, *Acta Phys. Pol. A* **123**, 513 (2013).

[34] M. Denys, M. Jagielski, T. Gubiec, R. Kutner, H. E. Stanley, *Acta Phys. Pol. A* **129**, 913 (2016).

[35] V. Gontis, S. Havlin, A. Kononovicius, B. Podobnik, H. E. Stanley, *arXiv:1507.05203* [q-fin.GN] (2015).

[36] V. Gontis, *Acta Phys. Pol. A* **129**, 1023 (2016).

[37] A. Corral, Physica A **340**, 590 (2004).